

AD-A152 374

PROTONATION AND LEWIS ACID-BASE EQUILIBRIA IN  
(BIPYRAZINE)MOLYBDENUM AND (U) YORK UNIV DOWNSVIEW  
(ONTARIO) DEPT OF CHEMISTRY E S DODWORTH ET AL. MAR 85

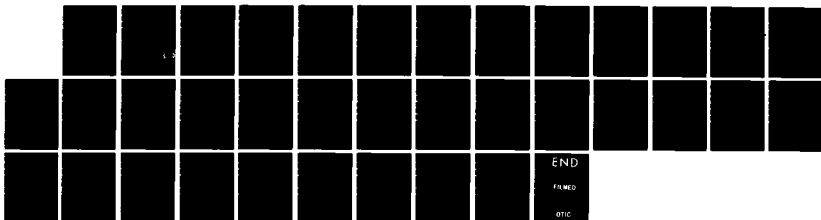
1/1

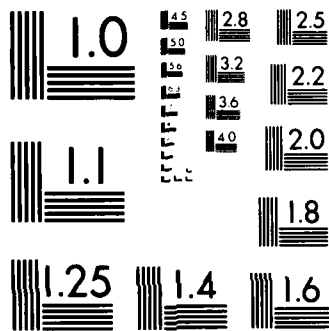
UNCLASSIFIED

TR-35 N00014-78-C-0592

F/G 7/4

NL





MICROCOPY RESOLUTION TEST CHART  
NATIONAL BUREAU OF STANDARDS 1963-A

2

OFFICE OF NAVAL RESEARCH

Contract N00014-78-C-0592

Task No. NR 051-693

TECHNICAL REPORT NO. 35

Protonation and Lewis Acid-Base Equilibria in (Bipyrazine)Molybdenum and  
(Bipyrazine)Tungsten Tetracarbonyls

BY

Elaine S. Dodsworth, A.B.P. Lever, Goran Eryavec and Robert J. Crutchley

Prepared for Publication

in

Inorganic Chemistry

York University

Department of Chemistry

Downsview (Toronto)

Ontario M3J-1P3

DTIC  
ELECTE  
APR 15 1985  
S D D

Reproduction in whole or in part is permitted for  
any purpose of the United States Government.

This document has been approved for public release  
and sale; its distribution is unlimited.

AD-A152 374

DTIC FILE COPY

REPORT DOCUMENTATION PAGE		READ INSTRUCTIONS BEFORE COMPLETING FORM	
1. REPORT NUMBER Technical Report No. 35	2. GOVT ACCESSION NO. <b>A152 374</b>	3. RECIPIENT'S CATALOG NUMBER	
4. TITLE (and Subtitle) Protonation and Lewis Acid-Base Equilibria in (Bipyrazine)Molybdenum and (Bipyrazine)Tungsten Tetracarbonyls		5. TYPE OF REPORT & PERIOD COVERED	
		6. PERFORMING ORG. REPORT NUMBER	
7. AUTHOR(s) Elaine S. Dodsworth, A.B.P. Lever, Goran Eryavec and Robert J. Crutchley		8. CONTRACT OR GRANT NUMBER(s)  N00014-78-C-0592	
		10. PROGRAM ELEMENT, PROJECT, TASK AREA & WORK UNIT NUMBERS	
9. PERFORMING ORGANIZATION NAME AND ADDRESS York University, Chemistry Department, 4700 Keele St., Downsview, Ontario M3J 1P3 Canada		12. REPORT DATE March, 1985	
11. CONTROLLING OFFICE NAME AND ADDRESS		13. NUMBER OF PAGES 28	
		15. SECURITY CLASS. (of this report)  Unclassified	
14. MONITORING AGENCY NAME & ADDRESS (if different from Controlling Office)		15a. DECLASSIFICATION/DOWNGRADING SCHEDULE	
16. DISTRIBUTION STATEMENT (of this Report) THIS DOCUMENT HAS BEEN APPROVED FOR PUBLIC RELEASE AND SALE;  ITS DISTRIBUTION IS UNLIMITED		Accession For NTIS GRA&I <input checked="" type="checkbox"/> DTIC TAB <input type="checkbox"/> Unannounced <input type="checkbox"/> Justification	
17. DISTRIBUTION STATEMENT (of the abstract entered in Block 20, if different from Report)		By Distribution/ Availability Codes Avail and/or Dist Special	
18. SUPPLEMENTARY NOTES  Prepared for publication in the Journal of Inorganic Chemistry		A-1	
19. KEY WORDS (Continue on reverse side if necessary and identify by block number)  Bipyrazine, Molybdenum, Tungsten, Carbonyl, Acid-base, Electronic spectra			
20. ABSTRACT (Continue on reverse side if necessary and identify by block number) The title complexes react with boron trifluoride etherate to generate mono- and di-BF <sub>3</sub> adducts. In H <sub>2</sub> SO <sub>4</sub> /ethanol solution one proton is coordinated. In each case reaction is assumed to occur at the peripheral uncoordinated nitrogen atoms of the bipyrazine unit. New metal to ligand charge transfer bands are observed for these various species. Analysis of the spectra shows that pK <sub>a</sub> (1) for the first uncoordinated nitrogen atom is about -0.3(Mo complex), and that extensive mixing of ground and excited states must be occurring to account for the oscillator strengths and bandwidths observed.			



Contribution from the Dept. of  
Chemistry, York University,  
Downsview (Toronto), Ontario,  
Canada M3J 1P3

Protonation and Lewis Acid-Base Equilibria in (Bipyrazine)Molybdenum and  
(Bipyrazine)Tungsten Tetracarbonyls

By Elaine S. Dodsworth, A.B.P. Lever\*, Goran Eryavec and Robert J. Crutchley

Abstract

The title complexes react with boron trifluoride etherate to generate mono- and di-BF<sub>3</sub> adducts. In H<sub>2</sub>SO<sub>4</sub>/ethanol solution one proton is coordinated. In each case reaction is assumed to occur at the peripheral uncoordinated nitrogen atoms of the bipyrazine unit. New metal to ligand charge transfer bands are observed for these various species. Analysis of the spectra shows that pK<sub>a</sub>(1) for the first uncoordinated nitrogen atom is about -0.3(Mo complex), and that extensive mixing of ground and excited states must be occurring to account for the oscillator strengths and bandwidths observed.

Introduction

Ground and excited state protonation equilibria involving the Ru(bpz)<sub>3</sub><sup>2+</sup> ion (bpz = bipyrazine) have recently been reported.<sup>1</sup> This species binds up to six protons in a step-wise fashion providing an interesting series of electronic absorption and emission data. Of especial interest was the variation in metal to ligand charge transfer (MLCT) energy as a function of the degree and site of protonation. Step-wise protonation provides a useful

mechanism for 'tuning' excited state redox potentials<sup>2</sup> and is of obvious interest in the design of photocatalytic redox reagents. Previous studies of protonation equilibria involving inorganic complexes have discussed protonation at the nitrogen atom of coordinated cyanide ion in species such as  $M(CN)_4L$  and  $M(CN)_2L_2$  ( $M = Fe, Ru$ ;  $L = di-imine$ )<sup>3,4</sup>, considered the enhanced acidity of ruthenium(II) complexes of 4,7-dihydroxy-1,10-phenanthroline<sup>5</sup>, and analysed the pH dependence of ruthenium bipyridine<sup>6</sup> and bipyrimidine<sup>7</sup> species. As is evident, much of the work has been associated with ruthenium or its congeners. The binding of Lewis acids to cyanide complexes and its effect on their charge transfer spectra has also been studied.<sup>8</sup> For these reasons we considered it useful to probe the protonation equilibria in a complex other than ruthenium and having only one bipyrazine unit to provide a data set which might be capable of more detailed analysis and additional insights.

The species  $M(CO)_4(bpz)$  ( $M = Mo, W$ )<sup>9</sup> are soluble in organic solvents and give rise to intense absorption in the visible region, attributed to metal to ligand charge transfer (MLCT)  $M \rightarrow bpz(\pi^*)$ . Addition of mineral acid, or the Lewis acid  $BF_3$  (etherate) causes changes in the visible absorption spectra which can be interpreted in terms of mono- and di-acid equilibria. FTIR and NMR data are reported in support of the equilibria proposed.

### Experimental

The complexes  $Mo(CO)_4(bpz)$  and  $W(CO)_4(bpz)$  were prepared according to literature methods.<sup>9</sup> Acetone and 96%  $H_2SO_4$  were BDH Analar grade. The acid was diluted using absolute ethanol. Boron trifluoride etherate was purified

according to a literature method<sup>10</sup> and stored under nitrogen or dry air. Electronic spectra were recorded on a Perkin-Elmer Hitachi Model 340 microprocessor spectrophotometer. The cell holder was cooled to ca. 10°C to minimise decomposition of the complexes. <sup>1</sup>H NMR spectra were recorded on a Varian EM360 60 MHz spectrometer at ambient temperature. Tetramethylsilane at 0.00 ppm or the residual protons of d<sub>6</sub>-acetone at 2.05 ppm were used as internal references. FTIR spectra were recorded on a Nicolet SX20 instrument, (courtesy of the Nicolet Co. of Canada) as acetone solutions in a sodium chloride cell. Computer simulations were obtained with a Commodore model 8032 microcomputer and an Epson MX80 matrix printer utilised in a plotting mode.

### Results and Discussion

The visible absorption spectra of the title species show two bands in the visible region, bands I and II (Tables I and II). These transitions have been studied previously<sup>9,11-16</sup> and are clearly associated with  $M(t_{2g}^6) \rightarrow bpz(b_2\pi^*)$  (MLCT I) and  $M(t_{2g}^6) \rightarrow bpz(a_2\pi^*)$  (MLCT II), being transitions from the metal d shell to the two lowest lying  $\pi^*$  orbitals of bpz. These are separated by some 7000-8000  $cm^{-1}$ .

The species show marked solvatochromic behaviour with the two MLCT transitions shifting to the blue by up to 3000  $cm^{-1}$  as the dielectric constant of the solvent is increased<sup>16</sup>, behaviour similar to the corresponding bipyridine (bipy) complexes.<sup>11,12</sup> There is indeed a simple linear correlation between the shifts of the MLCT transitions in  $M(CO)_4(bipy)$  with solvent, and those of the complexes under study here.<sup>16</sup> The presence of the two peripheral nitrogen atoms, absent in the bipyridine

species, was expected to cause deviations in the linear relationship between the two series, when acidic solvents were considered.

As far as glacial acetic acid and trichloroacetic acid (in ethanol) are concerned, no marked differences were noted and presumably protonation does not occur in these media. However, while the addition of mineral acids, HCl, HClO<sub>4</sub> and H<sub>2</sub>SO<sub>4</sub>, to an ethanolic solution of M(CO)<sub>4</sub>(bipy) causes only small solvatochromic shifts (to the blue) in the MLCT band energies, addition to M(CO)<sub>4</sub>(bpz) causes new bands to be observed.

Solutions of HCl, HClO<sub>4</sub>, and H<sub>2</sub>SO<sub>4</sub> in either water or ethanol cause gradual decomposition of the complexes, as indicated by a decrease in the intensity of the MLCT bands with time. The rate of decomposition increases with increasing acid concentration, being significant within minutes in 4M acid. We were not able to identify an acid system which was free of decomposition effects. Such decomposition also continues under an inert atmosphere (CO, N<sub>2</sub>). Solutions of H<sub>2</sub>SO<sub>4</sub> in ethanol were finally chosen for further study of the protonation since the complexes are readily soluble in this solvent, and decomposition is very slow at low acidities (<3M). Although some esterification must take place in the mixed EtOH/H<sub>2</sub>SO<sub>4</sub> medium, it does not seem to be a problem for our study, except that the proton concentration will be uncertain.

Addition of the Lewis acid, BF<sub>3</sub> (as boron trifluoride etherate), to solutions of the bpz complexes causes spectroscopic effects apparently similar to those of protonation. In both experiments the results for Mo and W complexes are qualitatively the same.

When boron trifluoride etherate is added dropwise to the, initially,

pink solution of  $M(\text{CO})_4(\text{bpz})$  ( $M = \text{Mo}, \text{W}$ ) in acetone, bands I (MLCT I) and II (MLCT II) diminish in intensity, and a new band (band Ia) appears at about 618 nm, shifting to lower energy with continued addition of the  $\text{BF}_3$ . Subsequently, at higher concentrations of the etherate, bands I and II essentially disappear and there remain band Ia and a new band at about 490 nm (band Ib). In pure boron trifluoride etherate as solvent, only bands Ia and Ib are seen, the latter being the more intense. These data are summarised in Table I and Fig. 1. When the solution is diluted, band Ib diminishes in intensity and bands I and II of the parent species reappear. Thus the reaction seems quite reversible with little or no decomposition.

Band Ia is associated with MLCT I of the mono- $\text{BF}_3$  adduct and band Ib with MLCT I of the di- $\text{BF}_3$  adduct. There is no evidence in the data obtained here for bands corresponding to MLCT II appearing in either adduct (at least to the red of the parent transition). The red shifting of band Ia, upon further addition of  $\text{BF}_3$  etherate, probably reflects a solvatochromic effect, expected to shift this transition to lower energies as the polar acetone is diluted with the less polar diethyl-ether.<sup>14</sup>

Attempts to isolate a solid adduct from reaction of  $\text{Et}_2\text{O} \cdot \text{BF}_3$  with  $\text{Mo}(\text{CO})_4\text{bpz}$  or  $\text{W}(\text{CO})_4\text{bpz}$  were unsuccessful; reactions of the solids with liquid  $\text{Et}_2\text{O} \cdot \text{BF}_3$  (at room temperature, in vacuo) produced black oils.

Data for protonation of  $\text{Mo}(\text{CO})_4\text{bpz}$  and  $\text{W}(\text{CO})_4\text{bpz}$  are presented in Table II and typical spectra are shown in Fig. 2. As the acidity of the solution is increased a new peak (band Ia) appears in the spectrum, red shifted with respect to MLCT I. Isosbestic points are observed at 586 and 584 nm for Mo

and W species respectively. Band Ia continues to increase in intensity (and also red shifts slightly), while MLCT I decreases. Above about 1.5M acid, the isosbestic point is lost, probably because decomposition is beginning to occur. Band I decreases to a shoulder in 2.5M H<sub>2</sub>SO<sub>4</sub>. Above this concentration a second new band (Ib) appears close to the position of MLCT I but significantly blue shifted. This band then increases in intensity relative to band Ia. At acid concentrations greater than 4M the rate of decomposition of the complex becomes significant relative to the time taken to record the spectrum; thus the investigation could not be continued.

The effect of acid on MLCT II, the  $d \rightarrow a_2\pi^*$  transition, is less easily observed due to its proximity to stronger bands in the UV region (bpz  $\pi \rightarrow \pi^*$  and M $\rightarrow$ CO MLCT) though it does show a decrease in intensity roughly parallel with MLCT I. No new bands are observed close to MLCT II. This absorption feature disappears altogether from the spectrum in >4M (Mo) and >3.25M (W) H<sub>2</sub>SO<sub>4</sub>.

When acid solutions ( $[H^+] < 1M$ ) are diluted or neutralised, bands I and II reappear and band Ia diminishes. However, if stronger acid solutions, in which band Ib is present, are diluted or neutralised, the reversal is incomplete and the spectra are broad in the region of band I. Furthermore if a solution in fairly strong acid is monitored with time, band Ib increases slightly over short time intervals (minutes) as band Ia decreases. This increase is not associated with growth in band II and cannot therefore reflect an increase in the concentration of the parent complex. Over longer time periods both bands Ia and Ib diminish. We return to this problem below.

Tetracarbonyldi-imine complexes of C<sub>2v</sub> symmetry have four allowed CO

stretching modes in their IR spectra:  $A_1$ ,  $B_1$ ,  $A_1$  and  $B_2$ . In  $\text{Mo}(\text{CO})_4\text{bpz}$  the two higher frequency bands correspond primarily to the trans carbonyls and the two lower bands primarily to the cis carbonyls.<sup>9,17,18</sup> FTIR spectra of the CO stretching region and corresponding electronic spectra were recorded for solutions of  $\text{Mo}(\text{CO})_4\text{bpz}$  in acetone and in the presence of varying amounts of  $\text{Et}_2\text{O}\cdot\text{BF}_3$ . Apart from some broadening of the CO bands as  $\text{BF}_3$  was added, there was no significant change in the spectrum during the growth of band Ia. When there was added a sufficient excess of  $\text{Et}_2\text{O}\cdot\text{BF}_3$  corresponding to the appearance of band Ib in the electronic spectrum, the energies of all four  $\nu(\text{CO})$  increased (Table III).

Assignments of the parent carbonyl spectrum (Table III) have already been discussed.<sup>9</sup> As expected for the CO band force constants,  $k_1$  (CO groups trans to di-imine)  $<$   $k_2$  (CO groups perpendicular to di-imine plane). We anticipate that boron trifluoridation will increase the acceptor power of the di-imine and lead to an increase in both  $k_1$  and  $k_2$ . The assignment shown in Table III for the  $\text{BF}_3$  adduct fulfills this expectation though the fit to the Kraihanzel-Cotton matrices<sup>18</sup> is not quite as good as for the parent species. This poorer fit probably reflects the fact that the dominant species in solution is the mono-adduct which possesses at best  $C_s$  symmetry, rather than the  $C_{2v}$  symmetry assumed by the theoretical analysis. Other assignments provide even poorer fits to the matrices or result in  $k_1 > k_2$ . This would imply that  $\text{bpzBF}_3$  is a better acceptor than CO which is an improbable result.

Note that these data permit one to derive the ligand effect constants defined by Timney for deducing carbon monoxide stretching force constants.<sup>19</sup>

The bpz and  $\text{BF}_3$  adduct may be compared with bipyridine and CO, as follows:-

	Cis constant	Trans constant
bipy	-24 $\text{N m}^{-1}$	-62 $\text{N m}^{-1}$
bpz	-13.5	-59
bpz $\text{BF}_3$	-5	-52.5
CO	33.5	126.1

The variation is consistent with the ligands becoming better  $\pi$ -acceptors in the sequence bipy < bpz < bpz $\text{BF}_3$  << CO.

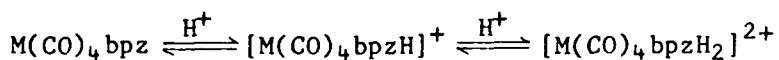
$^1\text{H}$  NMR spectra were recorded in acetone ( $d_6$ ) solution and in the presence of an excess of  $\text{Et}_2\text{O} \cdot \text{BF}_3$  (Table IV). The complex itself shows three resonances in the aromatic region.<sup>9</sup> On addition of  $\text{Et}_2\text{O} \cdot \text{BF}_3$  the same three resonances are observed, recognisable by their splitting patterns, but H3 and H6 are shifted downfield (H6 shows around twice the shift of H3) while H5 remains at almost the same position. These shifts can be interpreted in terms of a combination of several effects, as discussed by Martin et al.<sup>20</sup> who have recently reported the  $^1\text{H}$  NMR spectra of a series of substituted pyridines and their  $\text{BF}_3$  and  $\text{BBr}_3$  adducts.

The CO stretching frequency data for  $\text{Mo}(\text{CO})_4\text{bpz}$  (see above) indicate that the electron density on the metal decreases when the  $\text{BF}_3$  adduct is formed. This may be due to either weaker  $\sigma$  donation from the bpz or to increased  $\pi$  back-donation to the bpz, either one of which will add to the net deshielding of proton H6. Increased back-donation (and thus a net increase in ring current) seems more probable since this may explain why H3 shifts downfield when H5 does not, H3 being in a stronger field due to the  $\pi$  electrons of both rings.

The NMR data for  $\text{BF}_3$  addition appear to indicate that only one

(symmetric) species is present in solutions containing an excess of  $\text{Et}_2\text{O}\cdot\text{BF}_3$ . Since the reaction is reversible, it is possible that the rate of exchange of  $\text{BF}_3$  is fast on the NMR time scale so that an average signal is seen, due to the equilibrium between the mono- and di- $\text{BF}_3$  species.

The above results are interpreted in terms of a series of equilibria between the complex and the mono and di-adduct species. For example, in the case of protonation:



Band Ia is attributed to the MLCT transition in the monoprotonated complex. It increases in intensity as the acid concentration is increased and the equilibrium moves to the right, while bands I and II, due to the neutral species, decrease.

Approximate  $\text{pK}_a$  values may be calculated for the first protonation step where isosbestic points are present in the spectra. Values obtained at 283K (assuming  $[\text{H}^+] = [\text{H}_2\text{SO}_4]$ ) are around -0.3 for Mo and +0.1 for W complexes, though there is some variation in the apparent  $\text{pK}_a$  with acid concentration (due to experimental error and to other equilibria between the acid and solvent). These values are reasonable, lying between those of free bpz ( $\text{pK}_a = 0.45$ ) and  $[\text{Ru}(\text{bpz})_3]^{2+}$  ( $\text{pK}_a = -2.2$ )<sup>1</sup>. Although bonding to metal(0) might be expected to increase the  $\text{pK}_a$  of bpz, evidently back-bonding to the CO groups takes most of the M(0)  $\pi$  electron density.

The molecular orbitals of bipyrazine may be constructed by combining the orbitals of two pyrazine units in and out-of-phase, resulting in a low lying  $\pi^*$  orbital of  $b_2$  symmetry and a higher lying  $\pi^*$  orbital of  $a_2$  symmetry. This latter orbital is constructed of the  $a_{11}$   $\pi^*$  orbital of pyrazine (in

$D_{2h}$  symmetry), which possesses a nodal plane through the two nitrogen atoms.<sup>21</sup> It is likely that the dominant contribution to the bipyrazine  $a_2 \pi^*$  state also possesses nodal planes through the nitrogen atoms, providing a partial explanation of the differing effects of the initial protonation (or boron trifluoridation) upon the two MLCT transitions.

In the neutral species, the  $b_2 \pi^*$  orbital is symmetrically delocalised over the whole bipyrazine unit. In the monoprotinated species, this orbital will be stabilised by addition of a proton. A protonated bipyrazine unit may be created by combining pyz with  $\text{pyzH}^+$ . Although the symmetry is now lowered to  $C_s$ , two molecular orbitals corresponding to the original  $b_2 \pi^*$  and  $a_2 \pi^*$  of the neutral ligand are still obtained and we continue to use the same labels. The atomic orbital contributions to the molecular orbitals will be such that the  $\text{pyzH}^+$  moiety will contribute primarily to the lower energy  $b_2 \pi^*$ , while the  $a_2 \pi^*$  state is probably less perturbed and will still be roughly equally delocalised. The state corresponding to band Ia will therefore involve an electron localised mainly in the protonated pyrazine ring. Compare, for example, the red shift observed on protonation of pyrazine in  $[\text{Ru}(\text{NH}_3)_5(\text{pyz})]^{2+}$ .<sup>22</sup> The metal d orbitals are also expected to be stabilised somewhat as the protonated bpz becomes a stronger  $\pi$  acceptor (see below). The net red shift then corresponds to the difference in stabilisation of the metal and ligand ( $b_2 \pi^*$ ) orbitals.

The first nitrogen atom to be protonated in an excited bipyrazine unit is more basic in the excited state than in the ground state, due to the presence of the excited electron, resulting in a red shift of the MLCT transition (Forster).<sup>23</sup> The second excited state (MLCT II) is not a stronger

Fig 1

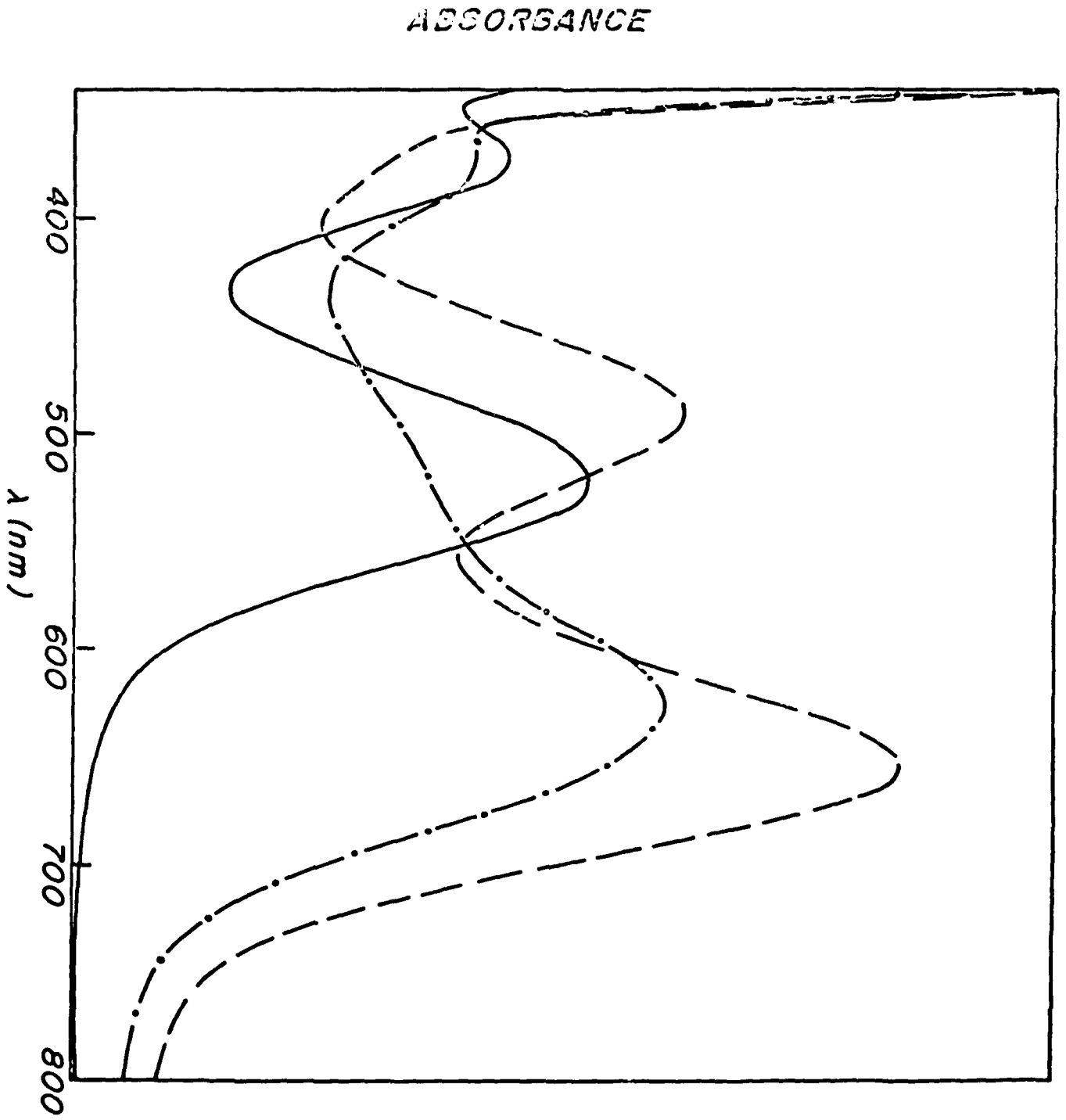


## FIGURE LEGENDS

### Figure 1

Visible absorption spectra of  $\text{Mo}(\text{CO})_4\text{bpz}$  showing the effect of  $\text{Et}_2\text{O}\cdot\text{BF}_3$  addition. \_\_\_\_\_ Initial spectrum in acetone. -.-.- Predominant species =  $\text{Mo}(\text{CO})_4\text{bpz}\cdot\text{BF}_3$ . --- Limiting spectrum corresponding (mainly) to

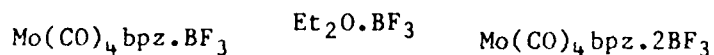


### Figure 2

(a) Visible absorption spectra of  $1 \times 10^{-4} \text{M}$   $\text{Mo}(\text{CO})_4\text{bpz}$  in  $\text{H}_2\text{SO}_4/\text{ethanol}$  as a function of  $[\text{H}_2\text{SO}_4]$ . Curves 1-5 correspond to  $[\text{H}_2\text{SO}_4]$  of 0, 0.5, 0.75, 1.0 and  $1.25 \text{ mol l}^{-1}$  respectively.  
(b) As (a) with  $[\text{H}_2\text{SO}_4] = 1.5\text{M}$  \_\_\_\_\_,  $2.0\text{M}$  -.-.-.-,  $2.5\text{M}$  -----.

### Figure 3

The simulated electronic spectra of  $\text{Mo}(\text{CO})_4\text{bpz}$  and its monoprotonated derivative. The spectra correspond with Fig. 2 (a) with the following percentage composition reading from the top spectrum at 377nm down. (i) 100% parent unprotonated; (ii) 92% parent, 8% monoprotonated; (iii) 86% parent, 14% monoprotonated; (iv) 81.55% parent, 17.95% monoprotonated, 0.5% 'diprotonated'; (v) (and lowest at 377 nm) 75% parent, 24% monoprotonated, 1% 'diprotonated'. The molar absorbances and bandwidths are as indicated in Table V; gaussian band shape was simulated.

### Figure 4

The gaussian construction of the spectrum labelled (v) in Fig. 3. The dotted lines correspond with the parent species, the circles to the monoprotonated species, and the crosses to the 'diprotonated' species.

**Table V** Spectroscopic Parameters

	Solvent	Transition	Energy ( $\epsilon$ )	Half Bandwidth	Oscillator Strength
Mo(CO) <sub>4</sub> bpz	A	MLCT I	18,300(7400)	2880	0.10
		MLCT Ix	20,700(<2000) <sup>a</sup>	2880 <sup>a</sup>	<0.03
		MLCT II	26,530(6160)	4550	0.13 <sup>b</sup>
Mo(CO) <sub>4</sub> bpz	B	MLCT I	19,230	3260	
		MLCT II	27,130	6200	
Mo(CO) <sub>4</sub> (bpzH) <sup>+</sup>	A (Ia)	MLCT I	15,650(12,580)	2340	0.13
Mo(CO) <sub>4</sub> (bpzBF <sub>3</sub> )	C (Ia)	MLCT I	15,400	2300	
Mo(CO) <sub>4</sub> (bpz(BF <sub>3</sub> ) <sub>2</sub> )	C (Ib)	MLCT I	20,400	6000	
W(CO) <sub>4</sub> bpz	A	MLCT I	17,920(9280)	2400	0.10
		MLCT II	26,200(6670)	3800	0.12 <sup>b</sup>
W(CO) <sub>4</sub> bpz	B	MLCT I	18,800	2800	
		MLCT II	27,000		
W(CO) <sub>4</sub> (bpzH) <sup>+</sup>	A (Ia)	MLCT I	15,750	1900	
W(CO) <sub>4</sub> (bpzBF <sub>3</sub> )	C (Ia)	MLCT I	15,630	1850	
W(CO) <sub>4</sub> (bpz(BF <sub>3</sub> ) <sub>2</sub> )	C (Ib)	MLCT I	20,400	4060	

A = EtOH, B = Acetone, C = Acetone/Ether/BF<sub>3</sub> Data in cm<sup>-1</sup>.

a) Estimated from deconvoluting MLCT I and MLCT Ix and fitting spectra.

b) Approximate; includes some contribution from uv region.

**Table IV.**  $^1\text{H}$  NMR Spectra of  $\text{Mo}(\text{CO})_4\text{bpz}$  and  $\text{W}(\text{CO})_4\text{bpz}^{\text{a}}$

	H3	H5	H6
$\text{Mo}(\text{CO})_4\text{bpz}$	10.05	8.90	9.27
+ $\text{Et}_2\text{O}\cdot\text{BF}_3$ (excess)	10.42	8.97	10.14
$\text{W}(\text{CO})_4\text{bpz}$	10.08	8.85	9.35
+ $\text{Et}_2\text{O}\cdot\text{BF}_3$ (excess)	10.41	8.80	10.19

(a) Data in ppm from  $\text{Me}_4\text{Si}$ . Recorded in  $d_6$  acetone.

Table III Carbonyl Stretching Frequencies and Force Constants<sup>a</sup>

	A <sub>1</sub>	B <sub>1</sub>	A <sub>1</sub>	B <sub>2</sub>	k <sub>1</sub>	k <sub>2</sub>	k <sub>f</sub>	A <sub>1</sub> (calc.)
Mo(CO) <sub>4</sub> bpz	2020	1919	1896	1851	14.17	15.55	0.34	1890
+ Et <sub>2</sub> O.BF <sub>3</sub> <sup>b</sup>	2024	1934 <sup>c</sup>	1921 <sup>c</sup>	1863	14.32	15.72	0.31	1890

a) Vibrational frequencies cited in cm<sup>-1</sup>, force constants in millidynes/Å. Solvent acetone. b) Note that the dominant species in the presence of excess Et<sub>2</sub>O.BF<sub>3</sub> is the mono-BF<sub>3</sub> adduct; however, some di-adduct will be present. c) The assignments of the 1934 and 1921 vibrations may be reversed. The reverse assignment leads to k<sub>1</sub> = 14.36, k<sub>2</sub> = 15.60, k<sub>f</sub> = 0.35 md/Å., A<sub>1</sub>(calc.) = 1891 cm<sup>-1</sup>.

**Table II.** (a) Spectroscopic Data for Mo(CO)<sub>4</sub>bpz in Ethanol/H<sub>2</sub>SO<sub>4</sub>

Concn. of H <sub>2</sub> SO <sub>4</sub> (mol l <sup>-1</sup> )	Band II		Band I/Ib		Band Ia	
	$\lambda_{\max}$ (nm)	$\epsilon$	$\lambda_{\max}$ (nm)	$\epsilon$	$\lambda_{\max}$ (nm)	$\epsilon$
0	377	6180	547	7430		
0.5	377	5880	542	6870	(sh)	
1.0	377	5350	542	6080	630	3340
1.5	377	5270	542	5610	634	4950
2.0	377	4800	546	5080	637	6560
2.5	377	4520	548(sh)	4850	640	7680
3.0	377	3800	540(sh)	4800	642	8860
3.5	376(sh)	3420	522	5980	647	9700
4.0	376(sh)	2660	522	7410	658	9630

(b) Spectroscopic Data for W(CO)<sub>4</sub>bpz in Ethanol/H<sub>2</sub>SO<sub>4</sub>

Concn. of H <sub>2</sub> SO <sub>4</sub> (mol l <sup>-1</sup> )	Band II		Band I/Ib		Band Ia	
	$\lambda_{\max}$ (nm)	$\epsilon$	$\lambda_{\max}$ (nm)	$\epsilon$	$\lambda_{\max}$ (nm)	$\epsilon$
0	380	6670	558	9280		
0.5	379	6470	554	8520	(sh)	
1.0	379	5980	556	7650	628	6600
1.5	379	4870	557	6700	631	8590
2.0	379	4690	560(sh)	6230	633	10280
2.5	380	4320	520,540(sh)	5720,6180	634	12320
3.0	380(sh)	3510	502,520(sh)	6960,6910	636	12620
3.5			506	9370	640	12910
4.0			503	10510	644	11680

$\epsilon$  = molar absorbance (l mol<sup>-1</sup> cm<sup>-1</sup>). (sh) = shoulder

Molar absorbances are not corrected for decomposition. Spectra were recorded immediately after mixing and errors are <2% for 2M H<sub>2</sub>SO<sub>4</sub> and <5% for 4M H<sub>2</sub>SO<sub>4</sub>.

Table I.

Electronic Spectra of  $M(\text{CO})_4\text{bpz}$  in the Presence of $\text{Et}_2\text{O}\cdot\text{BF}_3$ 

Approx. Concn. of $\text{Et}_2\text{O}\cdot\text{BF}_3$ (mol l <sup>-1</sup> )	Colour	$\text{Mo}(\text{CO})_4\text{bpz}$			$\text{W}(\text{CO})_4\text{bpz}$		
		II	$\lambda_{\text{max}}$ (nm) I/Ib	Ia	II	$\lambda_{\text{max}}$ (nm) I/Ib	Ia
0	pink	368.5	520		371	533	
0.07	pink	369	523	(sh)	371	534	(sh)
0.13	mauve	370	527	618	371	539	616
0.17	blue	371	(sh)	625	371	(sh)	620
0.20	blue	371	494	640	(sh)	482	630
0.33	grey-blue (sh)		490	653	-	480	640
7.9 <sup>a</sup>	grey-blue				322	490	654

Spectra recorded using approx.  $10^{-4}\text{M}$   $M(\text{CO})_4\text{bpz}$  in acetone. Solutions were deoxygenated with dry  $\text{N}_2$  before addition of  $\text{Et}_2\text{O}\cdot\text{BF}_3$ . (a) Complex dissolved in pure  $\text{Et}_2\text{O}\cdot\text{BF}_3$ .

- (17) Adams, D.M., "Metal-Ligand and Related Vibrations", Arnold, E., London, 1967, p.101.
- (18) Kraihanzel, C.S., Cotton, F.A., Inorg. Chem., 1963, 2, 533. Cotton, F.A., Kraihanzel, C.S., J. Am. Chem. Soc., 1962, 84, 4432.
- (19) Timney, J.A., Inorg. Chem., 1979, 18, 2502.
- (20) Martin, D.R., Mondal, J.U., Williams, R.D., Iwamoto, J.B., Massey, N.C., Nuss, D.M., Scott, P.L., Inorg. Chim. Acta., 1983, 70, 47.
- (21) Jorgenson, W.L., Salem, L., "The Organic Chemists Book of Orbitals", Academic Press, 1973.
- (22) Ford, P., Rudd, De F.P., Gaunder, R., Taube, H., J. Am. Chem. Soc., 1968, 90, 1187.
- (23) Ireland, J.F., Wyatt, P.A.H., Adv. Phys. Org. Chem., 1976, 12, 131.
- (24) Staal, L.H., Stufkens, D.J., Oskam, A., Inorg. Chim. Acta., 1978, 26, 255.
- (25) Lever, A.B.P., "Inorganic Electronic Spectroscopy", Elsevier Scientific Publ. Co., Amsterdam, 1968, 2nd. Ed. 1984, Chapter 4.

References

- (1) Crutchley, R.J., Kress, N., Lever, A.B.P., J. Am. Chem. Soc., **1983**, 105, 1170.
- (2) Haga, M-A., Dodsworth, E.S., Eryavec, G., Seymour, P., Lever, A.B.P., Inorg. Chem., Submitted for publication.
- (3) Schilt, A.A., J. Am. Chem. Soc. **1963**, 85, 904.
- (4) Peterson, S.H., Demas, J.N., J. Am. Chem. Soc., **1979**, 101, 6571.
- (5) Giordano, P.J., Bock, C.R., Wrighton, M.S., J. Am. Chem. Soc. **1978**, 100, 6960.
- (6) Giordano, P.J., Bock, C.R., Wrighton, M.S., Interrante, L.V., Williams, R.F.X., J. Am. Chem. Soc., **1977**, 99, 3187.
- (7) Hunziger, M., Ludi, A., J. Am. Chem. Soc., **1977**, 99, 7370.
- (8) Shriver, D.F., Posner, J., J. Am. Chem. Soc., **1966**, 88, 1672.
- (9) Crutchley, R.J., Lever, A.B.P., Inorg. Chem., **1982**, 21, 2276.
- (10) Perrin, D.D., Armarego, W.L.F., Perrin, D.R., "Purification of Laboratory Chemicals", 2nd. Edn., Pergamon Press, **1980**.
- (11) Saito, H., Fujita, J., Saito, K., Bull. Chem. Soc. Jpn., **1968**, 41, 863.
- (12) Burgess, J., J. Organomet. Chem., **1969**, 19, 218.
- (13) Walther, D., J. Prakt. Chem., **1974**, 316, 604.
- (14) Manuta, D.M., Lees, A.J., Inorg. Chem., **1983**, 22, 3825.
- (15) Balk, R.W., Stufkens, D.J., Oskam, A., Inorg. Chim. Acta., **1978**, , 28, 133.
- (16) Dodsworth, E.S., Lever, A.B.P., Eryavec, G., Crutchley, R.J., Inorg. Chem., To be submitted.

support. This work is part of a joint ONR Contract with Prof. A.J. Bard,  
(Austin).

contribution from valence bond forms of the type  $[\text{Mo}^+-\text{bpz}^-]$  which is also a description of the MLCT I excited state. Note that since MLCT I is primarily  $b_2 \rightarrow b_2^*$ , extensive mixing between ground and excited state is permitted by symmetry. A greater mixing of ground and excited state will lead to a smaller difference in bond lengths between these states, as is proposed. It will also lead to greater intensity, since the overlap between ground and excited state wavefunctions is obviously increased.<sup>25</sup>

The  $\text{BF}_3$  data support the conclusions reached on the basis of protonation. Band Ia, MLCT I in the mono- $\text{BF}_3$  species, is also more intense and narrower than MLCT I in the parent species (Table V). Band Ib, MLCT I in the di- $\text{BF}_3$  species, is apparently very strong and broad. Its high oscillator strength may be attributed to even greater mixing of metal and bpz orbitals caused by the strongly accepting nature of the two  $\text{BF}_3$  groups. The broadness may reflect significant splitting of the d ( $t_{2g}$  in  $O_h$ ) manifold since one of the three d orbitals ( $b_2$ ) is strongly favoured for mixing, and hence stabilisation relative to the other two.

In conclusion, the protonation and  $\text{BF}_3$  data provide evidence for significant mixing between metal and ligand orbitals and the stabilisation of a complex whose back-donating character may be very significant.

#### Acknowledgements

The authors are indebted to Prof. Ian M. Walker for useful discussions. We also wish to thank the Natural Sciences and Engineering Research Council (Ottawa) and the Office of Naval Research (Washington) for financial

we include a contribution from MLCT Ix, and a very small contribution from the decomposition product (band Ib) to achieve a good fit to the experimental data (Fig. 3). The molar intensity of MLCT Ix is assumed to be about 25% that of MLCT I; it cannot be much larger for then it would be revealed as a shoulder. It is assumed to have the same energy difference from MLCT I as observed in non-polar media. In this approximation, the intensity of band Ib is assumed to be the same as that of band Ia (MLCT I monoprotonated). Its inclusion in the calculated spectrum is necessary to shift the high energy tail of the band I absorption to higher energy with higher acidity. The half-bandwidth of band Ib was estimated from the high acidity data. The various parameters used to simulate the spectrum are shown in Table V. The agreement between calculated gaussian and observed spectra is amazingly good.

Because of the increased decomposition rate, it is not useful to try and simulate the spectra for higher acidities.

The data in Table V merit further consideration. Knowing the molar intensities and half-bandwidths, it is possible to estimate the oscillator strengths and these are also listed. The MLCT I transition in the monoprotonated species (band Ia) is definitively both narrower and much stronger than the corresponding band in the neutral species. The sharper transition provides evidence that the difference in ground and excited state equilibrium distances in this species is smaller than in the parent species. This fact probably reflects a greater degree of covalency in the Mo-N bond with enhanced back-donation because of the greater acceptor power of the now positively charged ligand. The ground state probably has a much greater

contain some contribution from the diprotonated species.

Despite this decomposition it is possible to obtain further useful information from the electronic spectra of the protonated species.

The molecular orbital analysis of this system has been discussed previously.<sup>15,24</sup> The low symmetry ( $C_{2v}$ ) causes complete loss of degeneracy in the metal d ( $t_{2g}$  in  $O_h$ ) orbitals, resulting in three possible  $d \rightarrow \pi^*$  transitions under the MLCT I (band I) envelope. In fact, only two of these are electronically allowed, and are evident in the spectra recorded in polar solvents as pronounced asymmetry in the band I envelope. In non-polar solvents where band narrowing occurs, the second transition appears as a weak higher energy shoulder.<sup>15,16,24</sup> The shoulder and band are assigned as the x-polarised  $a_2(d\pi) \rightarrow b_2(bpz\pi^*)$  (band Ix, MLCT Ix) and z-polarised  $b_2(d\pi) \rightarrow b_2(bpz\pi^*)$  (MLCT I) transitions respectively.<sup>15</sup>

Fig. 3 shows a computer simulation of the experimental data in Fig. 2a. The gaussians used are shown for one particular spectrum, in Fig. 4. The simulation was obtained in the following manner. The molar intensities and half-bandwidths of the parent species spectrum are known from the spectrum in ethanol. The existence of isosbestic points at low acidities and the comparatively large separation between the band I and band Ia peaks permits the estimation of the corresponding quantities for the monoprotinated species, assuming the absence of any diprotonated species, a good assumption at low acidity.

The spectra are then created using these data and the calculated percentages of parent and monoprotinated species derived from the experimental spectrum. In a second order correction of the calculated data,

base than the ground state since a red shifted band does not appear.<sup>23</sup> This is reasonable if the orbital indeed has nodal planes through the nitrogen atoms.

The well behaved nature of the spectra obtained with  $\text{BF}_3$ .etherate and the clean reversibility leave little doubt that band Ib in this experiment corresponds with the di- $\text{BF}_3$  adduct,  $\text{M}(\text{CO})_4(\text{bpz}(\text{BF}_3)_2)$ . This is blue shifted because the presence of one  $\text{BF}_3$  group, withdrawing electron density from the bpz ligand, will inhibit binding of the second. Thus the stability constant for binding the second  $\text{BF}_3$  unit in the excited state (formally bound to  $\text{Mo}(\text{I})$ ) is less than the corresponding value in the ground state (bound to  $\text{Mo}(\text{O})$ ); hence a blue shift in the Forster scheme.

Band Ib in the higher molarity  $\text{H}_2\text{SO}_4$  data is not so readily identified. The presence of one proton in the monoprotonated species will inhibit the binding of the second proton to a greater degree than in the  $\text{BF}_3$  situation, because of the added positive charge. The second  $\text{pK}_a$  value for free bipyrazine is -1.35, thus  $K_a(2)/K_a(1) = 63$ . This ratio is likely to prevail in the carbonyl complex. With this ratio,  $\text{pK}_a(2) = \text{ca } -2.0$  and essentially no (<5%) diprotonated complex would be seen even at the highest acid concentrations used in this study. Thus either band Ib is extraordinarily intense as MLCT I of the diprotonated species, or it is not associated with the diprotonated species. Since it increases slightly in intensity with time, and band I is not cleanly reproduced upon dilution or neutralisation, we suggest that band Ib arises at least in part, from a decomposition product. The band Ib envelope, however, probably does

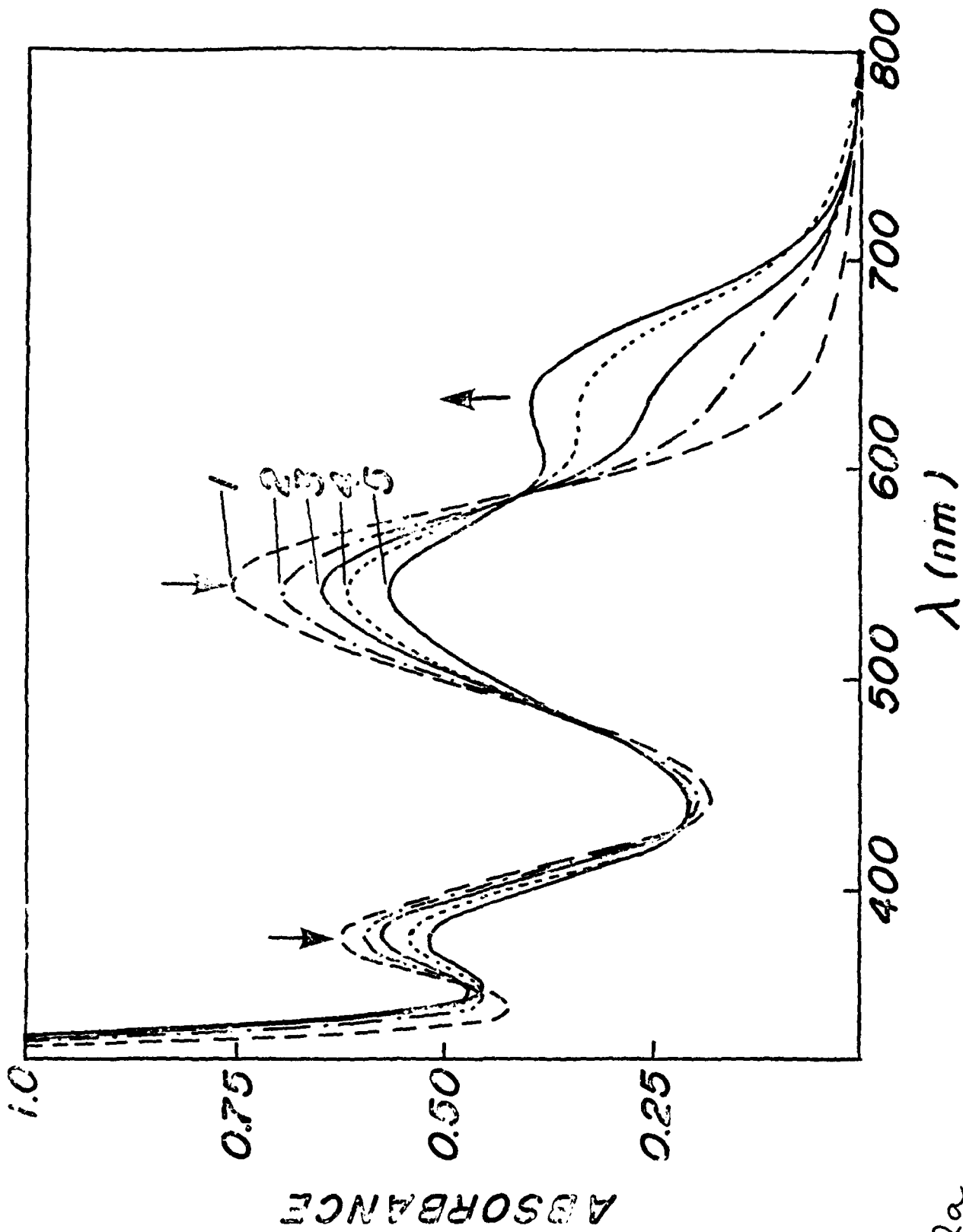


Fig 2a

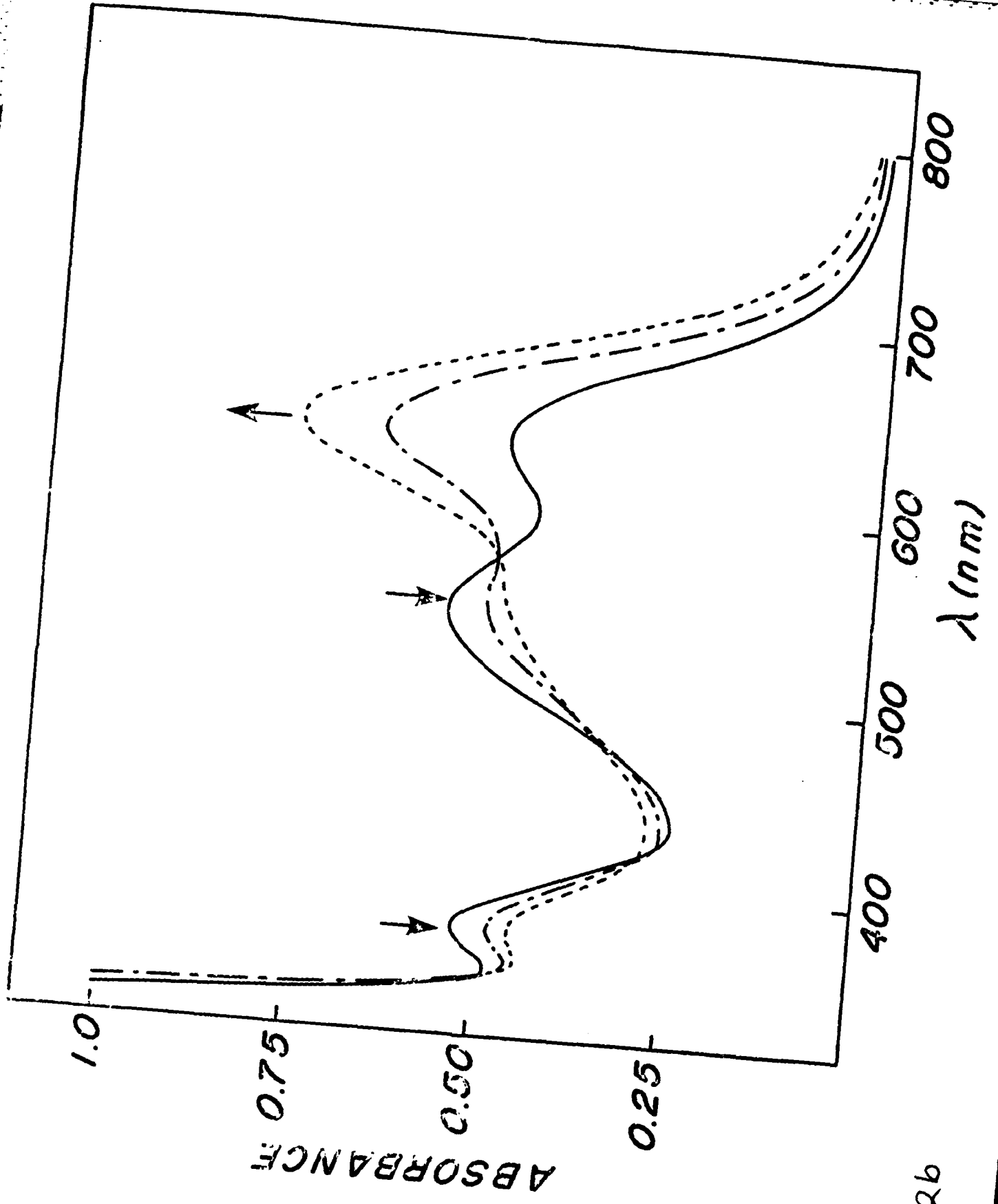


Fig 2b

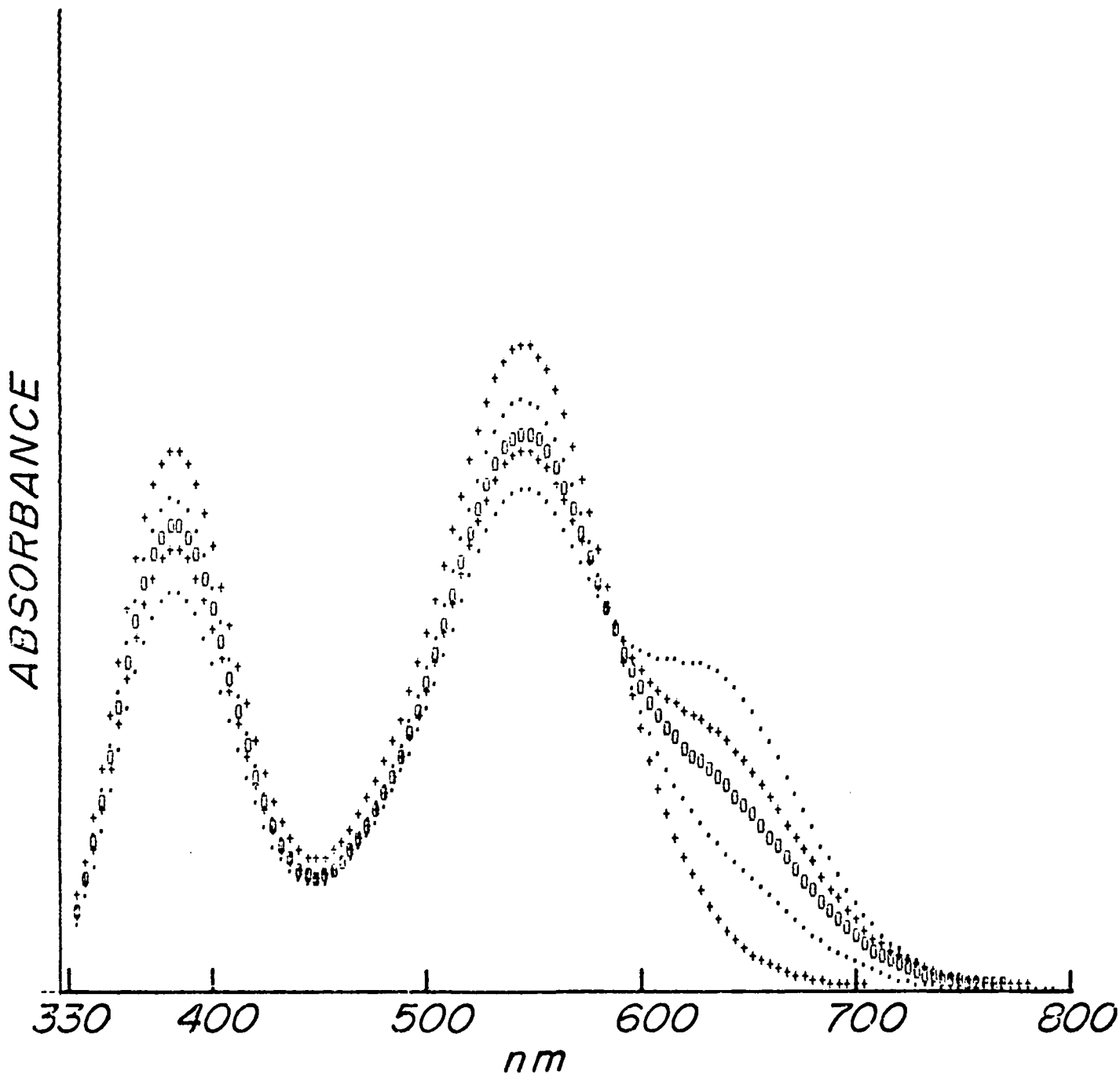


Fig 3.

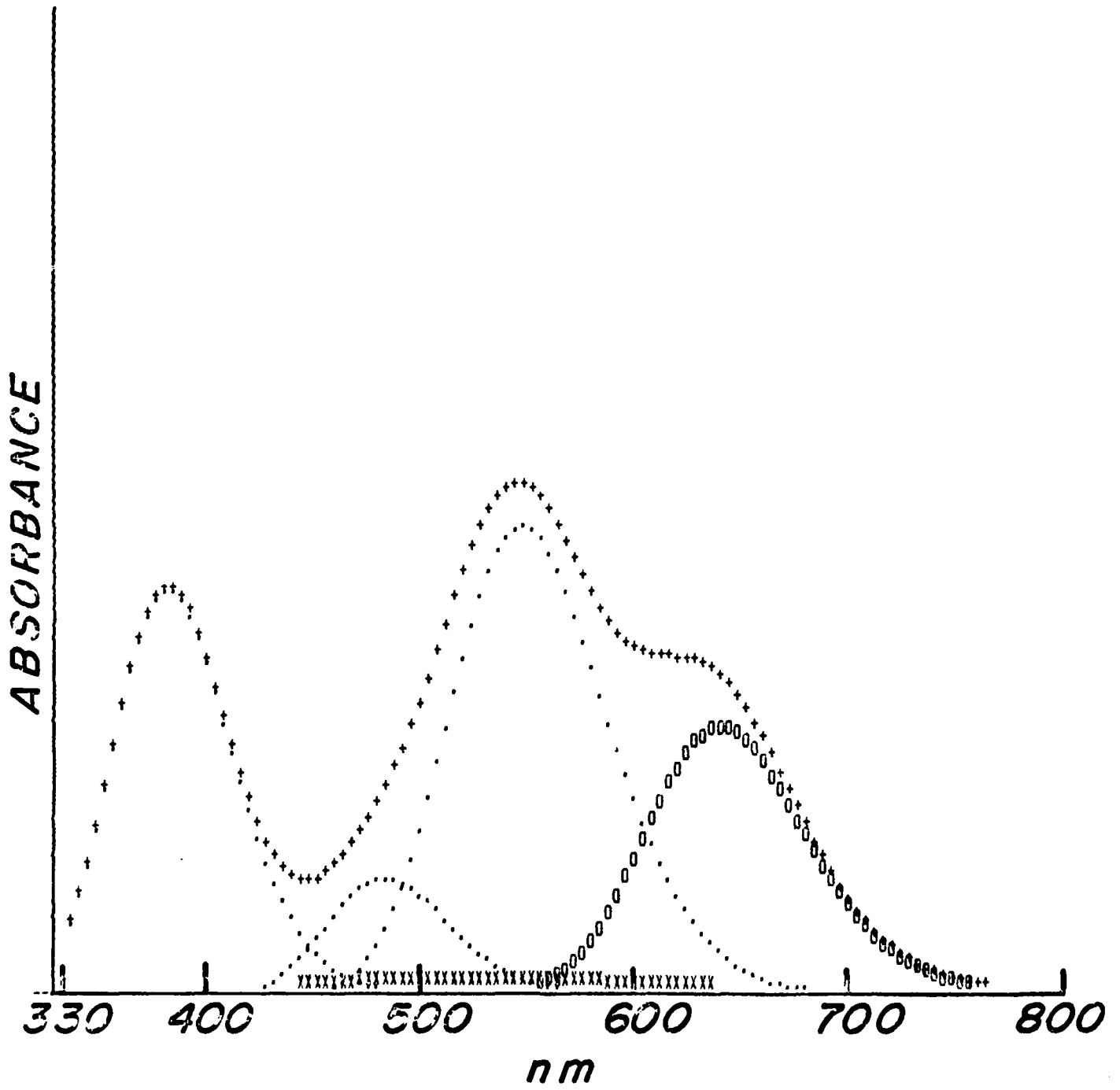


Fig 4.

TECHNICAL REPORT DISTRIBUTION LIST, GEN

	<u>No. Copies</u>		<u>No. Copies</u>
Office of Naval Research Attn: Code 413 800 N. Quincy Street Arlington, Virginia 22217	2	Dr. David Young Code 334 NORDA NSTL, Mississippi 39529	1
Dr. Bernard Doua Naval Weapons Support Center Code 5042 Crane, Indiana 47522	1	Naval Weapons Center Attn: Dr. A. B. Amster Chemistry Division China Lake, California 93555	1
Commander, Naval Air Systems Command Attn: Code 310C (H. Rosenwasser) Washington, D.C. 20360	1	Scientific Advisor Commandant of the Marine Corps Code RD-1 Washington, D.C. 20380	1
Naval Civil Engineering Laboratory Attn: Dr. R. W. Drisko Port Hueneme, California 93401	1	U.S. Army Research Office Attn: CRD-AA-IP P.O. Box 12211 Research Triangle Park, NC 27709	1
Defense Technical Information Center Building 5, Cameron Station Alexandria, Virginia 22314	12	Mr. John Boyle Materials Branch Naval Ship Engineering Center Philadelphia, Pennsylvania 19112	1
DTNSRDC Attn: Dr. G. Bosmajian Applied Chemistry Division Annapolis, Maryland 21401	1	Naval Ocean Systems Center Attn: Dr. S. Yamamoto Marine Sciences Division San Diego, California 91232	1
Dr. William Tolles Superintendent Chemistry Division, Code 6100 Naval Research Laboratory Washington, D.C. 20375	1		

ABSTRACTS DISTRIBUTION LIST, 359/627

Dr. Paul Delahay  
Department of Chemistry  
New York University  
New York, New York 10003

Dr. P. J. Hendra  
Department of Chemistry  
University of Southampton  
Southampton SO9 5NH  
United Kingdom

Dr. T. Katan  
Lockheed Missiles and  
Space Co., Inc.  
P.O. Box 504  
Sunnyvale, California 94088

Dr. D. N. Bennion  
Department of Chemical Engineering  
Brigham Young University  
Provo, Utah 84602

Mr. Joseph McCartney  
Code 7121  
Naval Ocean Systems Center  
San Diego, California 92152

Dr. J. J. Auburn  
Bell Laboratories  
Murray Hill, New Jersey 07974

Dr. Joseph Singer, Code 302-1  
NASA-Lewis  
21000 Brookpark Road  
Cleveland, Ohio 44135

Dr. P. P. Schmidt  
Department of Chemistry  
Oakland University  
Rochester, Michigan 48063

Dr. H. Richtol  
Chemistry Department  
Rensselaer Polytechnic Institute  
Troy, New York 12181

Dr. R. A. Marcus  
Department of Chemistry  
California Institute of Technology  
Pasadena, California 91125

Dr. E. Yeager  
Department of Chemistry  
Case Western Reserve University  
Cleveland, Ohio 44106

Dr. C. E. Mueller  
The Electrochemistry Branch  
Naval Surface Weapons Center  
White Oak Laboratory  
Silver Spring, Maryland 20910

Dr. Sam Perone  
Chemistry & Materials  
Science Department  
Lawrence Livermore National Laboratory  
Livermore, California 94550

Dr. Royce W. Murray  
Department of Chemistry  
University of North Carolina  
Chapel Hill, North Carolina 27514

Dr. B. Brummer  
EIC Incorporated  
111 Downey Street  
Norwood, Massachusetts 02062

Dr. Adam Heller  
Bell Laboratories  
Murray Hill, New Jersey 07974

Electrochimica Corporation  
Attn: Technical Library  
2485 Charleston Road  
Mountain View, California 94040

Library  
Duracell, Inc.  
Burlington, Massachusetts 01803

Dr. A. B. Ellis  
Chemistry Department  
University of Wisconsin  
Madison, Wisconsin 53706

Dr. Manfred Breiter  
Institut für Technische Elektrochemie  
Technischen Universität Wien  
9 Getreidemarkt, 1160 Wien  
AUSTRIA

ABSTRACTS DISTRIBUTION LIST, 359/627

Dr. M. Wrighton  
Chemistry Department  
Massachusetts Institute  
of Technology  
Cambridge, Massachusetts 02139

Dr. B. Stanley Pons  
Department of Chemistry  
University of Utah  
Salt Lake City, Utah 84112

Donald E. Mains  
Naval Weapons Support Center  
Electrochemical Power Sources Division  
Crane, Indiana 47522

S. Ruby  
DOE (STOR)  
M.S. 6B025 Forrestal Bldg.  
Washington, D.C. 20595

Dr. A. J. Bard  
Department of Chemistry  
University of Texas  
Austin, Texas 78712

Dr. Janet Osteryoung  
Department of Chemistry  
State University of New York  
Buffalo, New York 14214

Dr. Donald W. Ernst  
Naval Surface Weapons Center  
Code R-33  
White Oak Laboratory  
Silver Spring, Maryland 20910

Mr. James R. Moden  
Naval Underwater Systems Center  
Code 3632  
Newport, Rhode Island 02840

Dr. Bernard Spielvogel  
U.S. Army Research Office  
P.O. Box 12211  
Research Triangle Park, NC 27709

Dr. Aaron Fletcher  
Naval Weapons Center  
Code 3852  
China Lake, California 93555

Dr. M. M. Nicholson  
Electronics Research Center  
Rockwell International  
3370 Miraloma Avenue  
Anaheim, California

Dr. Michael J. Weaver  
Department of Chemistry  
Purdue University  
West Lafayette, Indiana 47907

Dr. R. David Rauh  
EIC Laboratories, Inc.  
111 Downey Street  
Norwood, Massachusetts 02062

Dr. Aaron Wold  
Department of Chemistry  
Brown University  
Providence, Rhode Island 02192

Dr. Martin Fleischmann  
Department of Chemistry  
University of Southampton  
Southampton SO9 5NH ENGLAND

Dr. R. A. Osteryoung  
Department of Chemistry  
State University of New York  
Buffalo, New York 14214

Dr. Denton Elliott  
Air Force Office of Scientific  
Research  
Bolling AFB  
Washington, D.C. 20332

Dr. R. Nowak  
Naval Research Laboratory  
Code 6170  
Washington, D.C. 20375

Dr. D. F. Shriver  
Department of Chemistry  
Northwestern University  
Evanston, Illinois 60201

Dr. Boris Cahan  
Department of Chemistry  
Case Western Reserve University  
Cleveland, Ohio 44106

ABSTRACTS DISTRIBUTION LIST, 359/627

Dr. David Aikens  
Chemistry Department  
Rensselaer Polytechnic Institute  
Troy, New York 12181

~~Dr. A. B. P. Lever  
Chemistry Department  
York University  
Downsview, Ontario M3J1P3~~

Dr. Stanislaw Szpak  
Naval Ocean Systems Center  
Code 6343, Bayside  
San Diego, California 95152

Dr. Gregory Farrington  
Department of Materials Science  
and Engineering  
University of Pennsylvania  
Philadelphia, Pennsylvania 19104

M. L. Robertson  
Manager, Electrochemical  
and Power Sources Division  
Naval Weapons Support Center  
Crane, Indiana 47522

Dr. T. Marks  
Department of Chemistry  
Northwestern University  
Evanston, Illinois 60201

Dr. Micha Tomkiewicz  
Department of Physics  
Brooklyn College  
Brooklyn, New York 11210

Dr. Lesser Blum  
Department of Physics  
University of Puerto Rico  
Rio Piedras, Puerto Rico 00931

Dr. Joseph Gordon, II  
IBM Corporation  
K33/281  
5600 Cottle Road  
San Jose, California 95193

Dr. Hector D. Abruna  
Department of Chemistry  
Cornell University  
Ithaca, New York 14853

Dr. D. H. Whitmore  
Department of Materials Science  
Northwestern University  
Evanston, Illinois 60201

Dr. Alan Bewick  
Department of Chemistry  
The University of Southampton  
Southampton, SO9 5NH ENGLAND

Dr. E. Anderson  
NAVSEA-56Z33 NC #4  
2541 Jefferson Davis Highway  
Arlington, Virginia 20362

Dr. Bruce Dunn  
Department of Engineering &  
Applied Science  
University of California  
Los Angeles, California 90024

Dr. Elton Cairns  
Energy & Environment Division  
Lawrence Berkeley Laboratory  
University of California  
Berkeley, California 94720

Dr. D. Cipris  
Allied Corporation  
P.O. Box 3000R  
Morristown, New Jersey 07960

Dr. M. Philpott  
IBM Corporation  
5600 Cottle Road  
San Jose, California 95193

Dr. Donald Sandstrom  
Boeing Aerospace Co.  
P.O. Box 3999  
Seattle, Washington 98124

Dr. Carl Kannewurf  
Department of Electrical Engineering  
and Computer Science  
Northwestern University  
Evanston, Illinois 60201

Dr. Richard Pollard  
Department of Chemical Engineering  
University of Houston  
4800 Calhoun Blvd.  
Houston, Texas 77004

ABSTRACTS DISTRIBUTION LIST, 359/627

Dr. Robert Somoano  
Jet Propulsion Laboratory  
California Institute of Technology  
Pasadena, California 91103

Dr. Johann A. Joebstl  
USA Mobility Equipment R&D Command  
DRDME-EC  
Fort Belvoir, Virginia 22060

Dr. Judith H. Ambrus  
NASA Headquarters  
M.S. RTS-6  
Washington, D.C. 20546

Dr. Albert R. Landgrebe  
U.S. Department of Energy  
M.S. 6B025 Forrestal Building  
Washington, D.C. 20595

Dr. J. J. Brophy  
Department of Physics  
University of Utah  
Salt Lake City, Utah 84112

Dr. Charles Martin  
Department of Chemistry  
Texas A&M University  
College Station, Texas 77843

Dr. H. Tachikawa  
Department of Chemistry  
Jackson State University  
Jackson, Mississippi 39217

Dr. Theodore Beck  
Electrochemical Technology Corp.  
3935 Leary Way N.W.  
Seattle, Washington 98107

Dr. Farrell Lytle  
Boeing Engineering and  
Construction Engineers  
P.O. Box 3707  
Seattle, Washington 98124

Dr. Robert Gotscholl  
U.S. Department of Energy  
MS G-226  
Washington, D.C. 20545

Dr. Edward Fletcher  
Department of Mechanical Engineering  
University of Minnesota  
Minneapolis, Minnesota 55455

Dr. John Fontanella  
Department of Physics  
U.S. Naval Academy  
Annapolis, Maryland 21402

Dr. Martha Greenblatt  
Department of Chemistry  
Rutgers University  
New Brunswick, New Jersey 08903

Dr. John Wasson  
Syntheco, Inc.  
Rte 6 - Industrial Pike Road  
Gastonia, North Carolina 28052

Dr. Walter Roth  
Department of Physics  
State University of New York  
Albany, New York 12222

Dr. Anthony Sammells  
Eltron Research Inc.  
4260 Westbrook Drive, Suite 111  
Aurora, Illinois 60505

Dr. W. M. Risen  
Department of Chemistry  
Brown University  
Providence, Rhode Island 02192

Dr. C. A. Angell  
Department of Chemistry  
Purdue University  
West Lafayette, Indiana 47907

Dr. Thomas Davis  
Polymer Science and Standards  
Division  
National Bureau of Standards  
Washington, D.C. 20234

Ms. Wendy Parkhurst  
Naval Surface Weapons Center R-33  
Silver Spring, Maryland 20910

**END**

**FILMED**

**5-85**

**DTIC**